Ultracold atoms with orbital angular momentum

A single ring for quantum sensing and a lattice of rings for quantum simulation

Jordi Mompart
Departament de Física, Universitat Autònoma de Barcelona

Atomtronics Workshop, Benasque, May 8, 2019

QUANTUM ATOM OPTICS GROUP (UAB)

http://grupsderecerca.uab.cat/qaos/

Juan Luis Rubio, Josep Cabedo, Gerard Pelegrí, Verònica Ahufinger, Jordi Mompart, Ramón Corbalán, Gerard Queraltó, Todor Kirilov

J. Polo
(now in Okinawa)

A. Turpin
(now in Glasgow)

Ultracold atoms
- Quantum transport
- Atomtronics in ring traps
- Orbital angular momentum states
- Complex tunneling and edge states

Laser-matter interaction
- Sub-wavelength localization and nanoscopy
- Atomic frequency combs
- Spin-orbit coupling

Light propagation in coupled optical waveguides
- Dark and bright OAM modes
- SUSY techniques for mode filtering

Conical Refraction
- Fundamentals: theory and experiment
- Applications: trapping microparticles and BECs

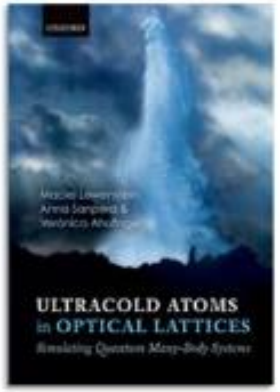

Ultracold Atoms in Optical Lattices
Simulating Quantum Many-Body Systems

Maciej Lewenstein, Anna Sanpera, and Verònica Ahufinger

Oxford University Press (2012)

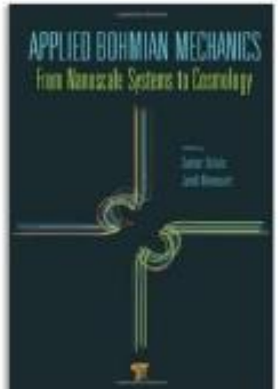

Applied Bohmian Mechanics
From Nanoscale Systems to Cosmology

Eds: Xavier Oriols and Jordi Mompart

Pan Stanford Publishing (2012)

BEC + OAM + Ring trap

See also the talks by Charles Clark and Mark Baker in Atomtronics 2019.

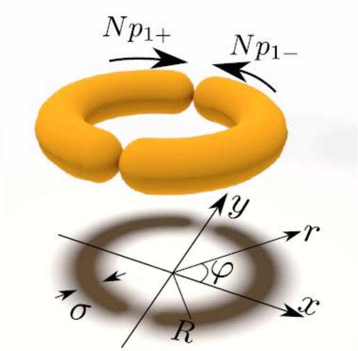

Quantum sensing using imbalanced counter-rotating BEC modes

G. Pelegrí, J. M., and V. Ahufinger, New Journal of Physics **20**, 103001 (2018)

- Magnetic fields with BECs are measured by using stimulated Raman transitions [1], performing Bragg interferometry after free fall [2], measuring Larmor precession in spinor BECs [3], or looking at density fluctuations [4].

- Rotations with BECs can be measured taking profit of the Sagnac effect [5], with ring geometries being specially well suited for this purpose [6].

[1] M. L. Terraciano *et. al.*, *Opt. Express* 16, 13062 (2008).
[2] K.S. Hardman *et. al.*, *Phys. Rev. Lett.* 117, 138501 (2016).
[3] Y. Eto *et. al.*, *Phys. Rev. A* 88, 031602(R) (2013).
[4] F. Yang *et. al.*, *Phys. Rev. Applied* 7, 034026 (2017).
[5] B. Barrett *et. al.*, *Comptes Rendus Physique* 15, 875 (2014).
[6] P. Navez *et. al.*, *New J. Phys.* 18, 075014 (2016).

See also the posters by G. Pelegrí *et al.*, and by D. Pfeiffer *et al.*, in Atomtronics 2019.

Ultracold atoms + OAM + Two rings + Tunneling

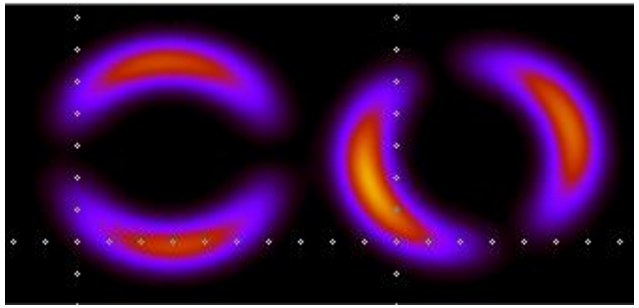

Geometrically induced complex tunneling with OAM states

J. Polo, J. M., Verònica Ahufinger, Phys. Rev. A **93**, 033613 (2016)

Suitable forcing of the optical lattice
P. Windpassinger *et al.*,
Phys. Rev. Lett. **108**, 225304 (2012)

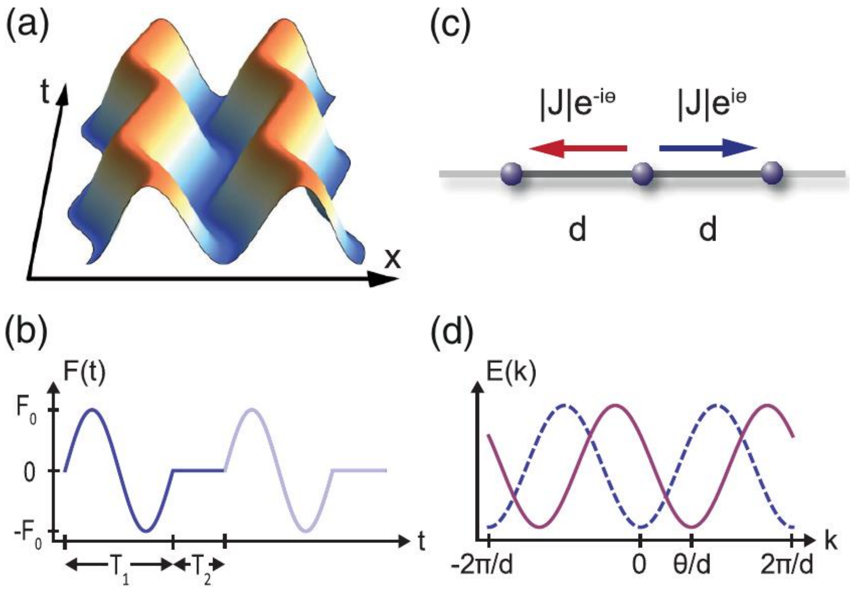

Combination of radio frequency and Raman fields that couple to the internal states of the atom
I. B. Spielman *et al.*, Phys. Rev. Lett. **108**, 225303 (2012)

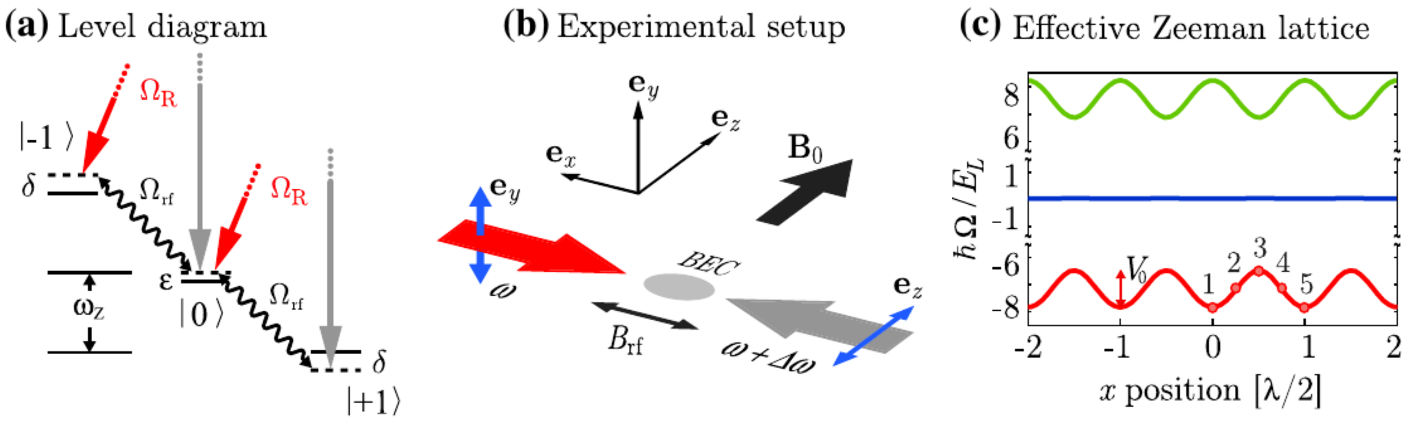

See also the talk by David Guéry-Odelin in Atomtronics 2019

Ultracold atoms + OAM + Lattice of rings + Tunneling

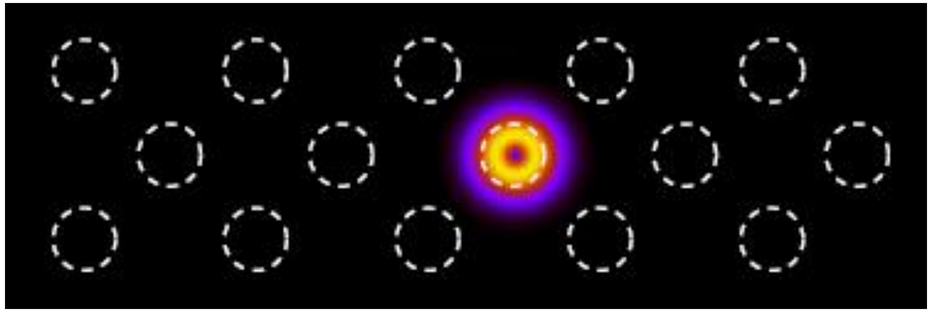

Topological edge states with ultracold atoms carrying OAM
G. Pelegrí, A. Marques, R. Dias, A. Daley, V. Ahufinger, J. M. Phys. Rev. A **99**, 023612 (2019)

Aharanov-Bohm caging with ultracold atoms carrying OAM
G. Pelegrí, A. Marques, R. Dias, A. Daley, J. M., V. Ahufinger, Phys Rev A **99**, 023613 (2019)

Complex tunnelings play a key role in quantum simulation. To cite a few examples, the realization of the Hofstader [1], XY spin [2], and Haldane [3] models. Through the syntetic dimension approach [4], demonstration of chiral edge states in bosonic [5] and fermion [6] ladders.

See also the talks by Roberta Citro and by Matteo Rizzi, and the poster by T. Haug *et al.*, in Atomtronics 2019

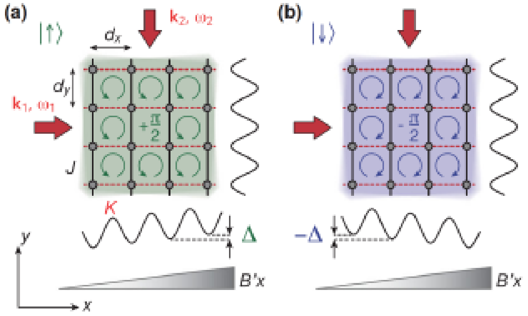

[1] M. Aidelsburger, *et. al.*, Phys. Rev. Lett. **111**, 185301 (2013).

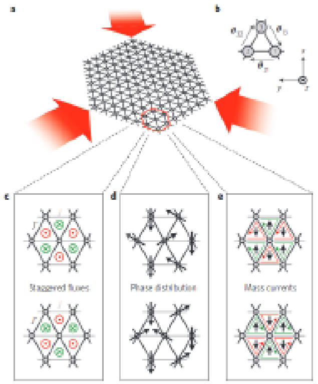

[2] J. Struck, *et. al.*, Nat. Phys. **9**, 738 (2013).

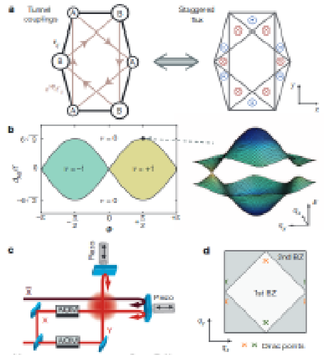

[3] G. Jotzu, *et. al.*, Nature **515**, 237 (2014).

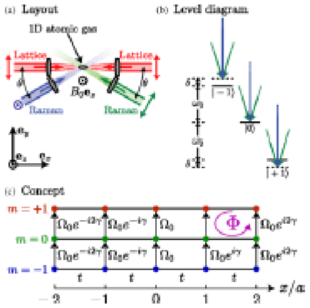

[4] A. Celi, *et. al.*, Phys. Rev. Lett., **112**, 043001 (2014).

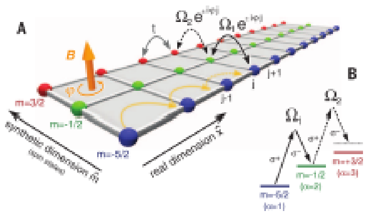

[5] M. Mancini, *et. al.*, Science **349**, 1510 (2015).

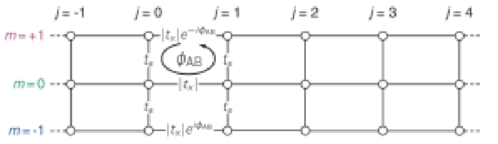

[6] B. K. Stuhl, *et. al.*, Science **349**, 1514 (2015).

A single ring for quantum sensing

- Two-dimensional BEC with *N* atoms in a ring trap

OAM states: $\langle \vec{r} | l, \pm \rangle = \phi_{l\pm}(\vec{r}) = \phi_{l\pm}(r, \varphi) = f(r) e^{\pm i l \varphi}$

Initial state: imbalanced superposition of $l = \pm 1$ states

$$\Psi(\vec{r}, t=0) = \sqrt{p_{1+}}\phi_{1+}(\vec{r}) + \sqrt{p_{1-}}\phi_{1-}(\vec{r})$$
$$= f(r)\left(\sqrt{p_{1+}}e^{i\varphi} + \sqrt{p_{1-}}e^{-i\varphi}\right)$$

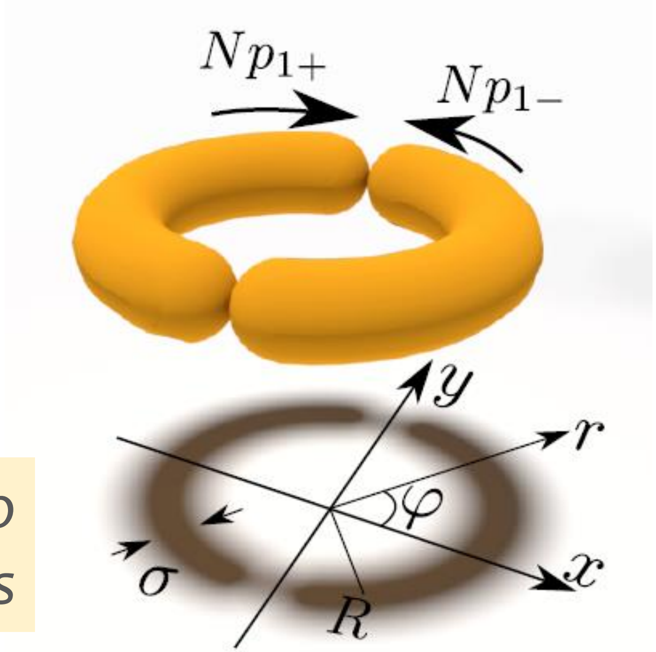

The density profile has a <u>minimal density line</u> due to quantum interference between the counter-rotating modes

A single ring for quantum sensing

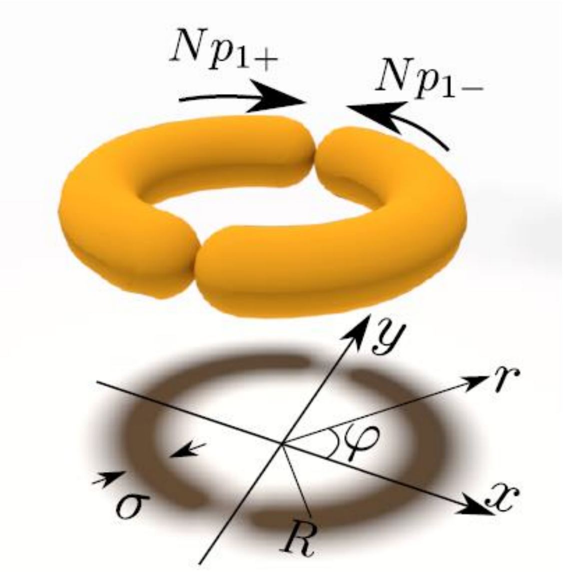

- Numerical integration of the 2D GPE

Ring potential in the *x*-*y* plane: $V(r) = \frac{1}{2} m\omega^2 (r - R)^2$

Harmonic potential in z: $\omega_z \gg \omega$

Time and space units: $1/\omega$ and $\sigma = \sqrt{\frac{\hbar}{m\omega}}$

Dimensionless 2D GPE (mean-field regime):

$$i\frac{\partial \Psi}{\partial t} = H\Psi = \left[-\frac{\nabla^2}{2} + V(r) + g_{2d}|\Psi|^2\right]\Psi$$

with $g_{2d} = Na_s\sqrt{\frac{8\pi m\omega_z}{\hbar}}$

Example: $R = 5,\ g_{2d} = 1,\ p_{1+} = 0.7$

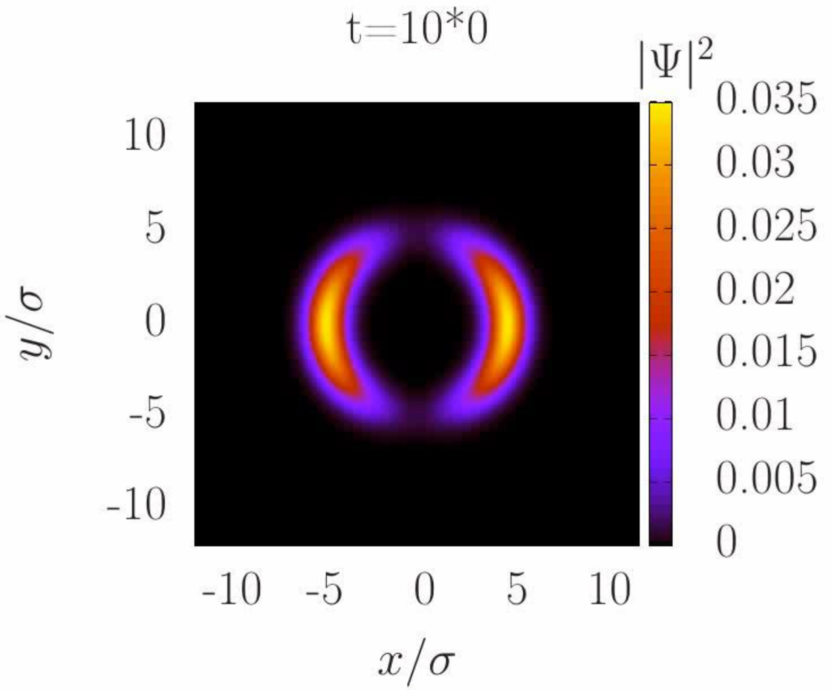

A single ring for quantum sensing

Example: $R = 5,\ g_{2d} = 1,\ p_{1+} = 0.7$

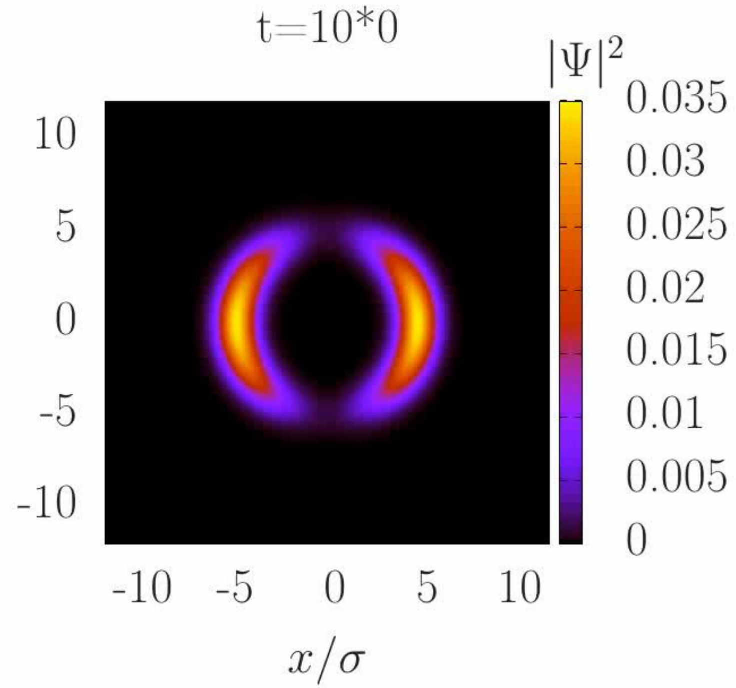

Evolution of the populations:

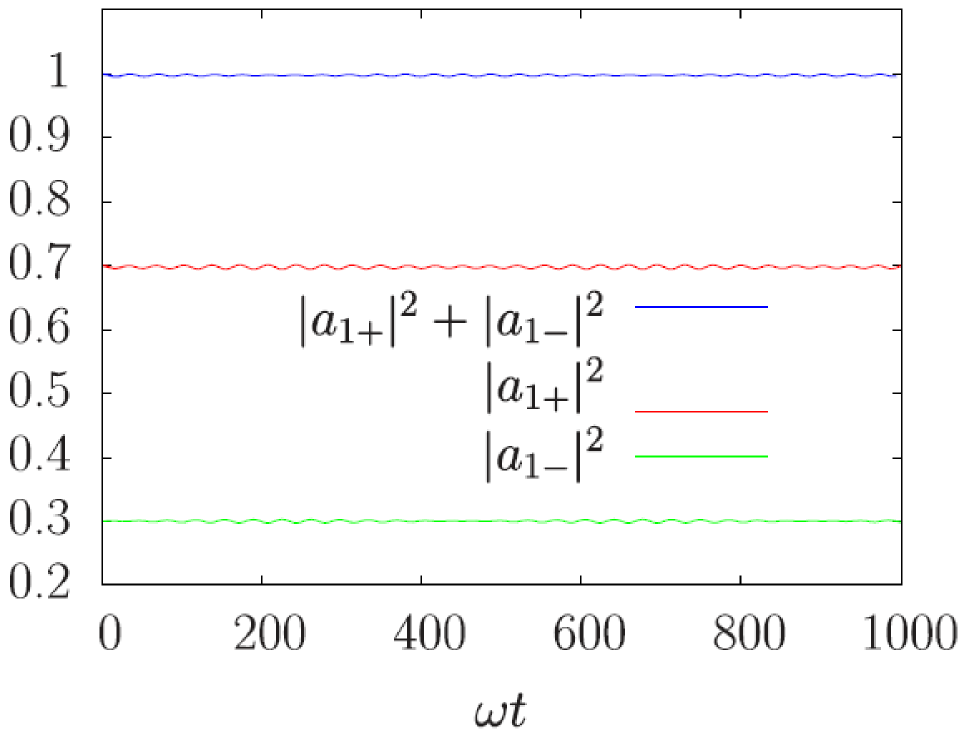

The <u>minimal density line</u> rotates at a constant speed, which depends on g_{2d}, and the populations of the OAM modes remain almost constant

A single ring for quantum sensing

- Expansion of the BEC wavefunction in OAM modes

Ansatz: $\Psi = \sum_m a_m(t)\phi_m(r,\varphi)$

Non-linear coupled equations: $$i\frac{da_l}{dt} = \mu_l a_l + U\sum_{m\neq m'} a_m a^*_{m'} a_{(l+m'-m)}$$

with $U = g_{2d}\int |f(r)|^4 d\vec{r} \equiv g_{2d}\mathcal{I}$ and $H\phi_l(\vec{r}) = \mu_l\phi_l(\vec{r})$

The dynamics does not couple odd with even OAM modes

For small g_{2d} values, a four state model (FSM) with $|l|=1,3$ is enough to reproduce the previously shown 2D GPE simulations

A single ring for quantum sensing

Example: $R = 5,\ g_{2d} = 1,\ p_{1+} = 0.7$

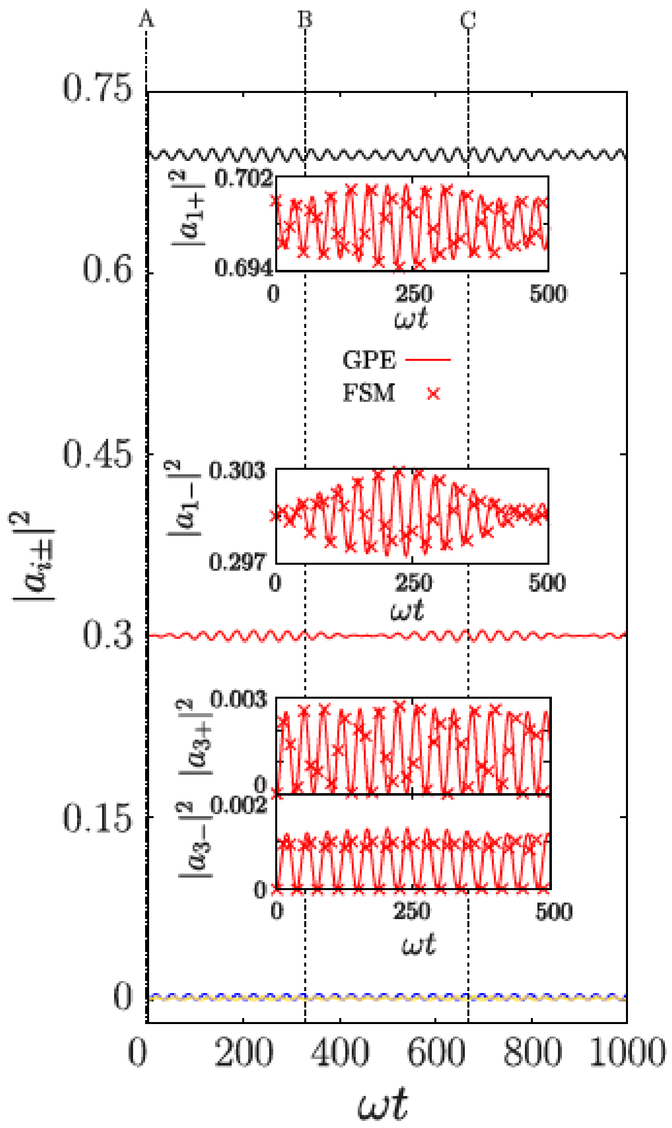

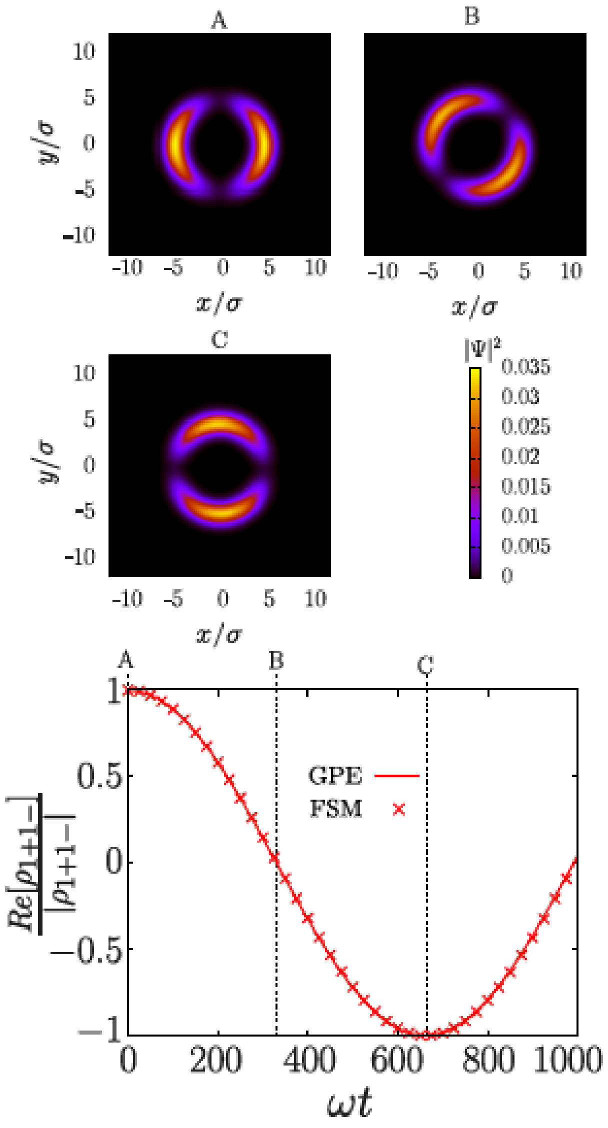

In the regime $U \ll (\mu_3 - \mu_1)$

assuming

$$|a_{1+}|^2 = p_{1+} = ct,\ |a_{1-}|^2 = p_{1-} = ct$$

and neglecting $\mathcal{O}(a_{3\pm}^2)$

Rotation frequency of the minimal density line

$$\Omega_{\mathrm{FSM}} = \frac{U(p_{1+} - p_{1-})}{2\left(1 + \frac{U}{\mu_3 - \mu_1}\right)}$$

$$U = g_{2d} \int |f(r)|^4 d\vec{r} \equiv g_{2d}\mathcal{I}$$

$$H\phi_l(\vec{r}) = \mu_l \phi_l(\vec{r})$$

A single ring for quantum sensing

- Sensing of two-body interactions

Rotation frequency of the minimal density line

$$\Omega_{\mathrm{FSM}} = \frac{U(p_{1+} - p_{1-})}{2(1 + \frac{U}{\mu_3 - \mu_1})}$$

$$U = g_{2d} \int |f(r)|^4 d\vec{r} \equiv g_{2d}\mathcal{I}$$

$$H\phi_l(\vec{r}) = \mu_l \phi_l(\vec{r})$$

$$g_{2d} = \frac{1}{\mathcal{I}} \frac{2\Omega}{(p_{1+} - p_{1-}) - 2\frac{\Omega}{\mu_3 - \mu_1}}$$

All the quantities on the right hand side can be measured by imaging the density profile of the BEC. Experimental protocol presented in Pelegrí et al., NJP ***20****, 103001 (2018).*

A single ring for quantum sensing

Comparative between 2D GPE simulations and the FSM

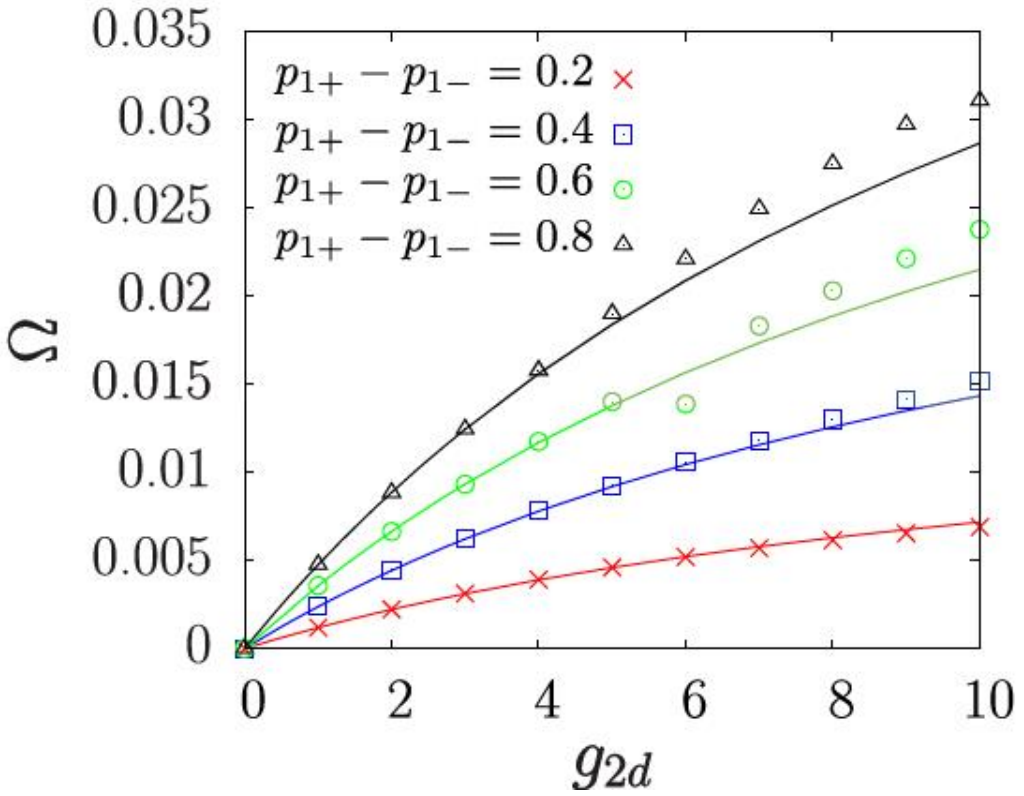

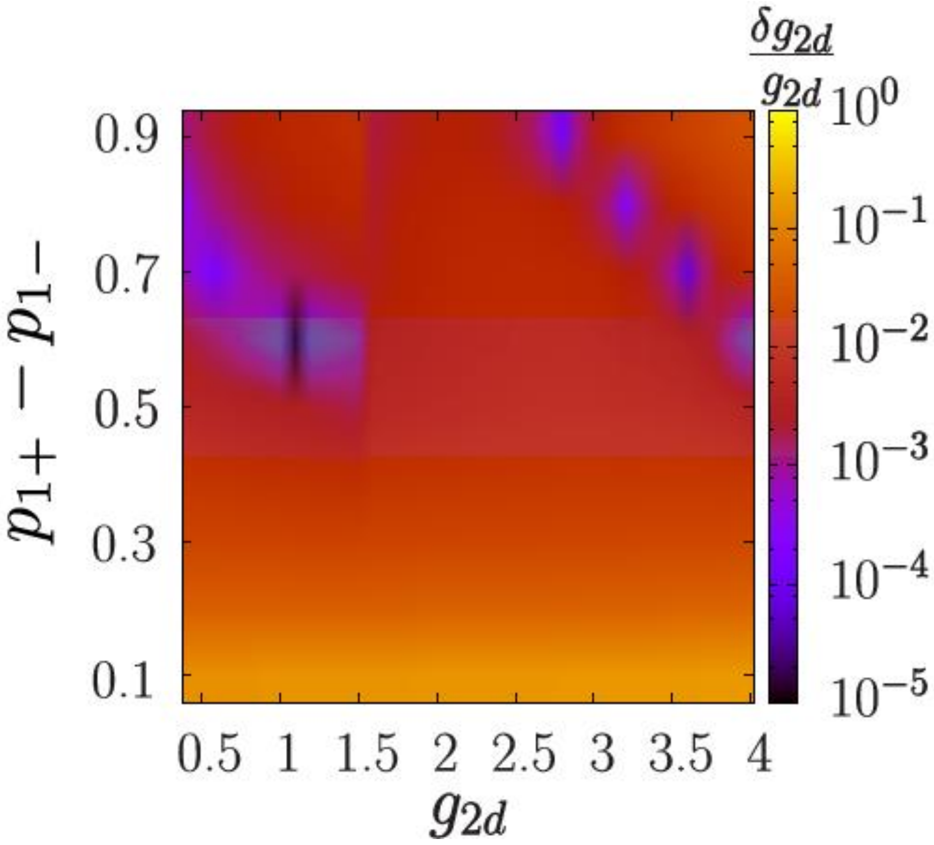

A single ring for quantum sensing

- Sensing of magnetic fields

Assume that the scattering length a_s can be manipulated with an external magnetic field *B*, e.g., close to a Feshbach resonance.

Then, $g_{2d} = Na_s\sqrt{\frac{8\pi m\omega_z}{\hbar}}$ and $U = g_{2d}\int |f(r)|^4 d\vec{r} \equiv g_{2d}\mathcal{I}$ will be also *B*-dependent.

Recalling that $\Omega_{\text{FSM}} = \dfrac{U(p_{1+} - p_{1-})}{2(1 + \frac{U}{\mu_3 - \mu_1})}$

Then:

$$\boxed{\frac{d\Omega_{\text{FSM}}}{dB} = \frac{(p_{1+} - p_{1-})\mathcal{I}N\sqrt{\frac{8\pi m\omega_z}{\hbar}}}{2(1 + \frac{U(B)}{(\mu_3 - \mu_1)})^2}\frac{da_S}{dB}}$$

$$\boxed{\Delta B_{\text{th}} = \frac{\sqrt{\frac{8\hbar}{\pi m\omega_z}}}{(p_{1+} - p_{1-})\mathcal{I}N}\frac{1}{\frac{da_S}{dB}}\Delta\Omega.}$$

A single ring for quantum sensing

- Sensing of rotations

In a frame rotating at an angular speed Ω_{ext}, the dimensionless 2D GPE reads:

$$i\frac{\partial \Psi}{\partial t} = \left[-\frac{\nabla^2}{2} + V(r) + g_{2d}|\Psi|^2 + i\Omega_{\mathrm{ext}}\hbar\frac{\partial}{\partial \varphi}\right]\Psi$$

Ω_{ext} can be measured as the difference between the measured speed, Ω, and the one expected from the FSM expression, Ω_{FSM}

$$\Omega_{ext} = \Omega - \Omega_{FSM}$$

Two rings: complex tunneling from OAM states

- One atom with localized OAM in two tunnel-coupled identical cylindrically symmetric potentials

winding number

$$\Psi_j^{\ell}(r_j,\phi_j)=\langle\vec{r}\,|\,j,\ell\,\rangle=\psi(r_j)e^{i\ell(\phi_j-\phi_0)}$$

j=L,R

azymuthal phase origin

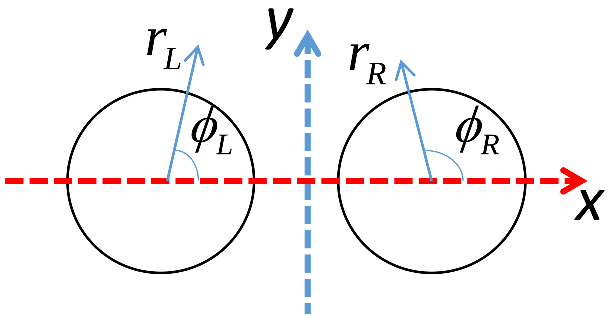

<u>Example</u>: single atom in the left trap with $\ell=1$

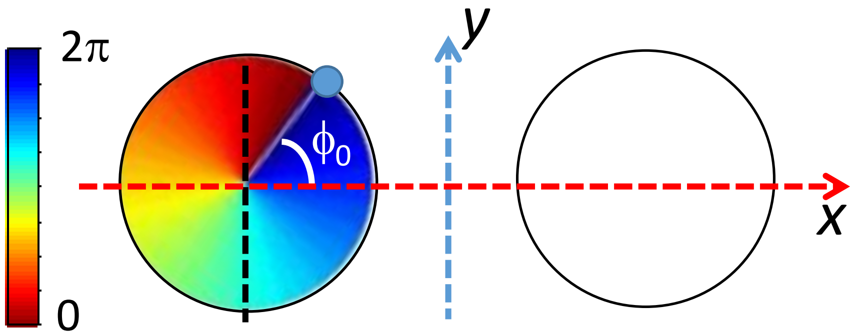

$$\Psi_L^1(r_L,\phi_L)=\Psi_L^1(\phi_0=0)e^{-i\phi_0}$$

Two rings: complex tunneling from OAM states

Symmetries for two tunnel-coupled identical cylindrically symmetric potentials

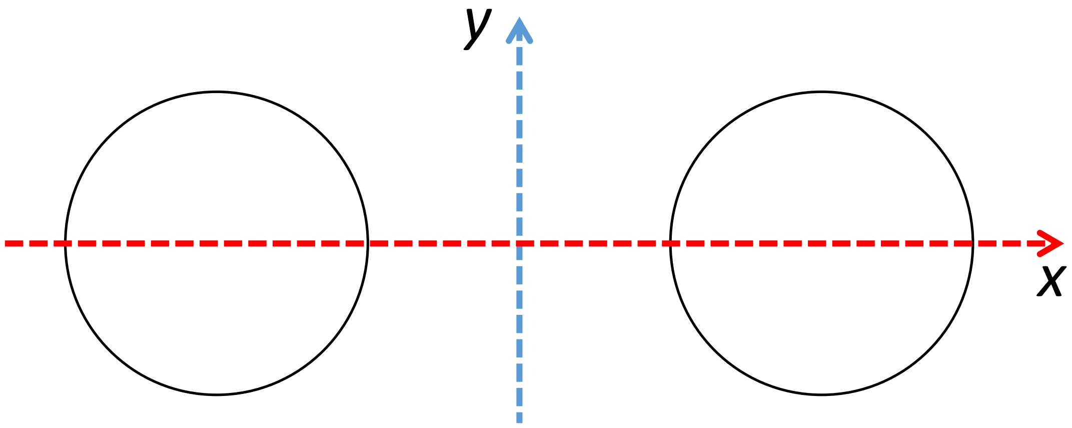

Two symmetries for *V*(*x*,*y*):

x-Mirror $M_x : y \leftrightarrow -y$

y-Mirror $M_y : x \leftrightarrow -x$

$$H\Psi(x,y,t) = \left[-\frac{\hbar^2}{2m}\nabla_\perp^2 + V(x,y) \right]\Psi(x,y,t)$$

$$[H, M_x] = [H, M_y] = 0$$

The trapping potential and, therefore, the Hamiltonian are invariant under the *x*- and *y*-mirror transformations

Tunneling amplitudes

$$J_{j.n}^{k,p} = \langle k,p|H|j,n\rangle = \langle k,p|M_y^{-1}M_yH|j,n\rangle = \langle k,p|M_y^{-1}HM_y|j,n\rangle$$

…in an analogous way for the mirror M_x

j,*k* = L,R *n*,*p* = winding number

How do they transform?

Two rings: complex tunneling from OAM states

<u>Example</u>: single atom in the left trap with *m* = 1, i.e., $\left| L,1 \right\rangle$

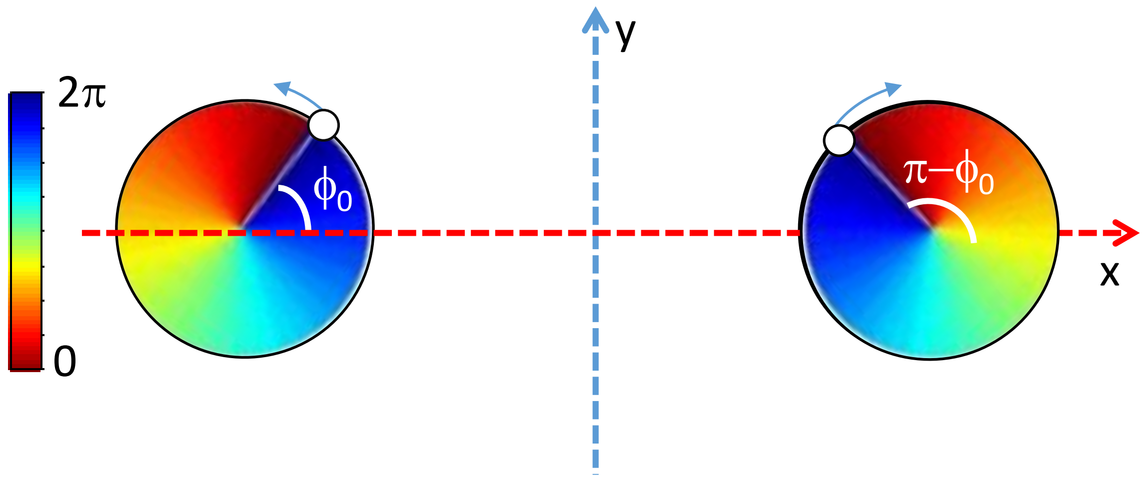

y-mirror: $x \leftrightarrow -x$

$$M_y \left| L,1 \right\rangle = \left| R,-1 \right\rangle e^{i(\pi-\phi)_0} e^{-i\phi_0} = -\left| R,-1 \right\rangle e^{-2i\phi_0}$$

x-Mirror: $y \leftrightarrow -y$

$$M_x \left| L,1 \right\rangle = \left| L,-1 \right\rangle e^{-2i\phi_0}$$

j,k = L,R *n,p* = winding number

$$J^{k,p}_{j.n} = \left\langle k,p \right| H \left| j,n \right\rangle = \left\langle k,p \right| M_y^{-1} H M_y \left| j,n \right\rangle$$

$$= \left\langle k,p \right| M_x^{-1} H M_x \left| j,n \right\rangle$$

$$J^{k,p}_{j.n} = \left(J^{j,n}_{k.p} \right)^* \quad \text{Hermiticity}$$

For n,p = ±ℓ

$J^{L,-\ell}_{L,\ell} = |J^{L,-\ell}_{L,\ell}| e^{2i\ell\phi_0} \longrightarrow J_1$

$J^{R,\ell}_{L,\ell} \longrightarrow J_2$

$J^{R,-\ell}_{L,\ell} = |J^{R,-\ell}_{L,\ell}| e^{2i\ell\phi_0} \longrightarrow J_3$

Two rings: complex tunneling from OAM states

Tunneling amplitudes as a function of the traps separation d (in harmonic oscillator units)

Each trap potential: $V(r) = \frac{1}{2} m\omega^2 (r - R)^2$

For $|\ell| = 1$

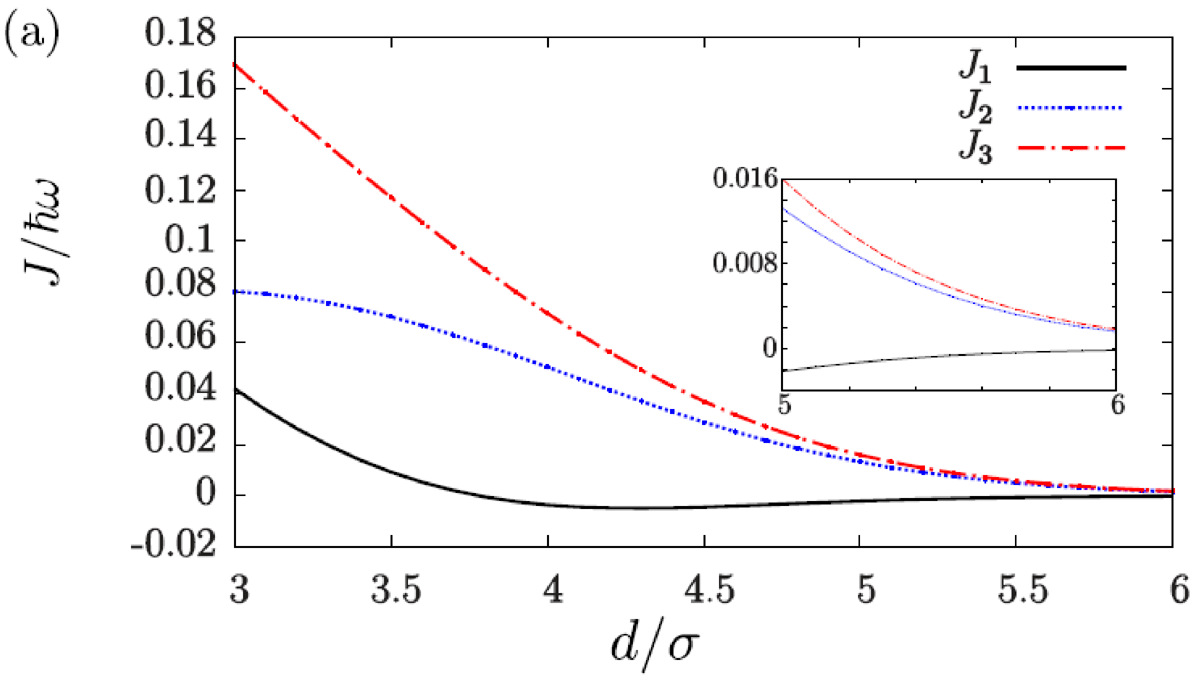

R = 0 (2D harmonic potentials)

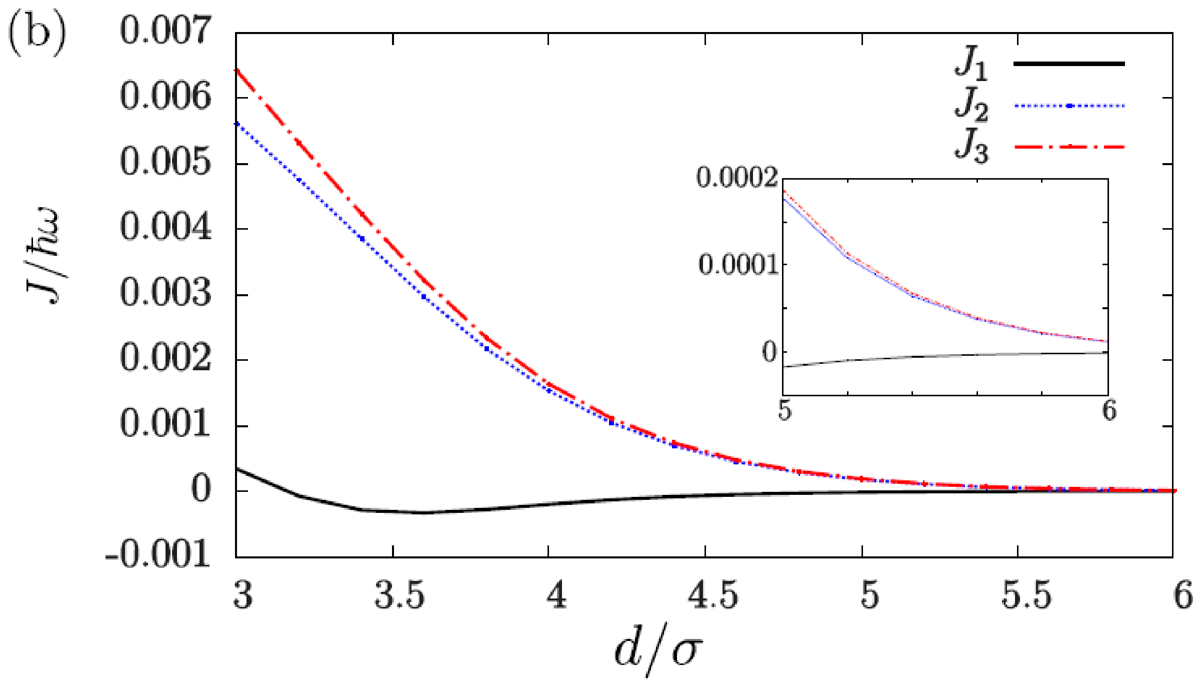

R = 5σ

Three rings: complex tunnelings from OAM states

For $|\ell| = 1$

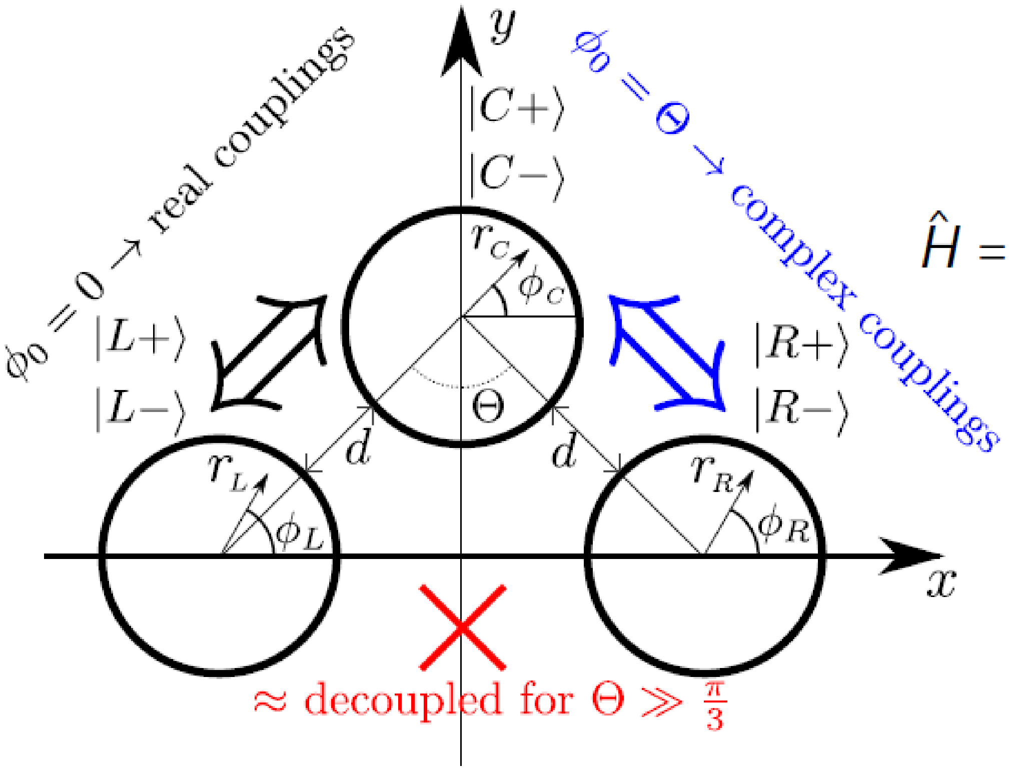

$$\hat{H} = \hbar \begin{pmatrix} 0 & J_1 & J_2 & J_3 & 0 & 0 \\ J_1 & 0 & J_3 & J_2 & 0 & 0 \\ J_2 & J_3 & 0 & J_1(1+e^{-2i\Theta}) & J_2 & J_3 e^{-2i\Theta} \\ J_3 & J_2 & J_1(1+e^{2i\Theta}) & 0 & J_3 e^{2i\Theta} & J_2 \\ 0 & 0 & J_2 & J_3 e^{-2i\Theta} & 0 & J_1 e^{-2i\Theta} \\ 0 & 0 & J_3 e^{2i\Theta} & J_2 & J_1 e^{2i\Theta} & 0 \end{pmatrix}$$

where $\begin{bmatrix} |L+\rangle \\ |L-\rangle \\ |C+\rangle \\ |C-\rangle \\ |R+\rangle \\ |R-\rangle \end{bmatrix}$ and $J_1 = J_{L,1}^{L,-1}$, $J_2 = J_{L,1}^{C,1}$, $J_3 = J_{L,1}^{C,-1}$

A lattice of rings for quantum simulation

Ultracold gas of non-interacting particles in a quasi-1D optical lattice with a diamond chain geometry.
Atoms loaded into the manifold of $|l| = 1$ OAM states.

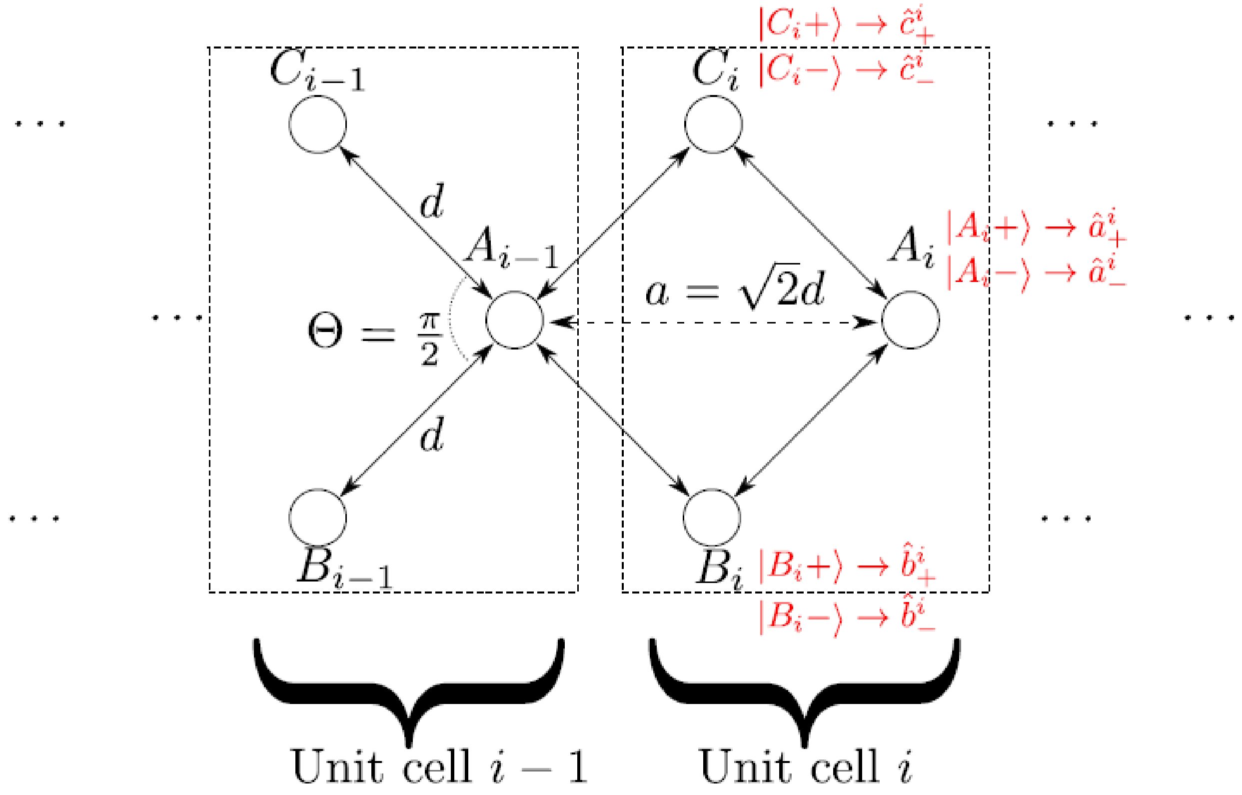

$$\hat{\Psi} = \sum_{i}^{\text{cells}} \sum_{\alpha=\pm} \Phi_\alpha^{a_i}(r_{a_i}, \phi_{a_i})\hat{a}_\alpha^i + \Phi_\alpha^{b_i}(r_{b_i}, \phi_{b_i})\hat{b}_\alpha^i + \Phi_\alpha^{c_i}(r_{c_i}, \phi_{c_i})\hat{c}_\alpha^i \qquad \text{with} \quad \phi_\alpha^{j_i}(r_{j_i}, \phi_{j_i}) = \langle \vec{r} | j_i, \pm \rangle$$

A lattice of rings for quantum simulation

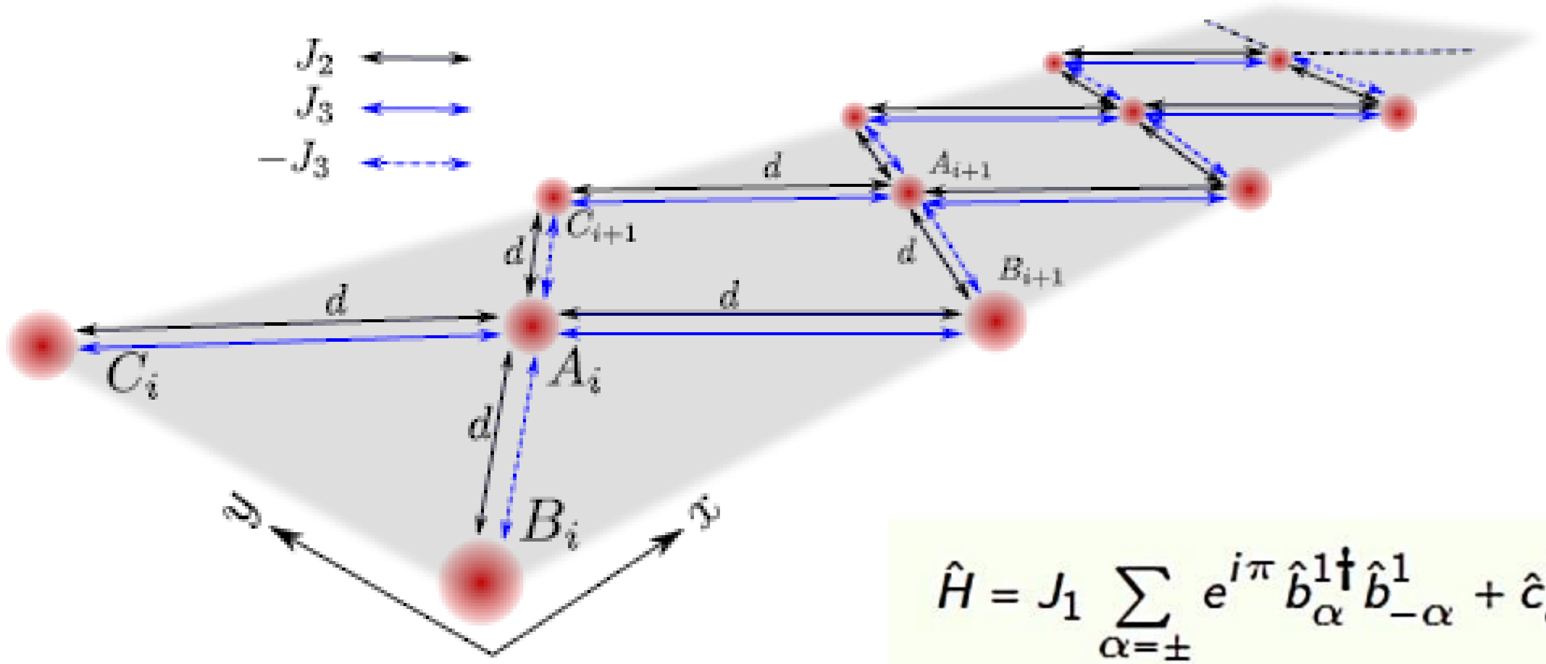

$$\hat{H} = J_1 \sum_{\alpha=\pm} e^{i\pi}\, \hat{b}^{1\dagger}_{\alpha}\hat{b}^{1}_{-\alpha} + \hat{c}^{1\dagger}_{\alpha}\hat{c}^{1}_{-\alpha}$$

$$+ J_2 \sum_{i=1}^{N_C}\sum_{\alpha=\pm}\left[\hat{a}^{i\dagger}_{\alpha}(\hat{b}^{i}_{\alpha} + \hat{b}^{i+1}_{\alpha} + \hat{c}^{i}_{\alpha} + \hat{c}^{i+1}_{\alpha})\right] + \text{h.c.}$$

$$+ J_3 \sum_{i=1}^{N_C}\sum_{\alpha=\pm}\left[\hat{a}^{i\dagger}_{\alpha}(e^{i\pi}\,\hat{b}^{i}_{-\alpha} + \hat{b}^{i+1}_{-\alpha} + \hat{c}^{i}_{-\alpha} + e^{i\pi}\,\hat{c}^{i+1}_{-\alpha})\right] + \text{h.c.}$$

A lattice of rings for quantum simulation

- Band structure

Six states per unit cell → six energy bands, which appear in degenerate pairs

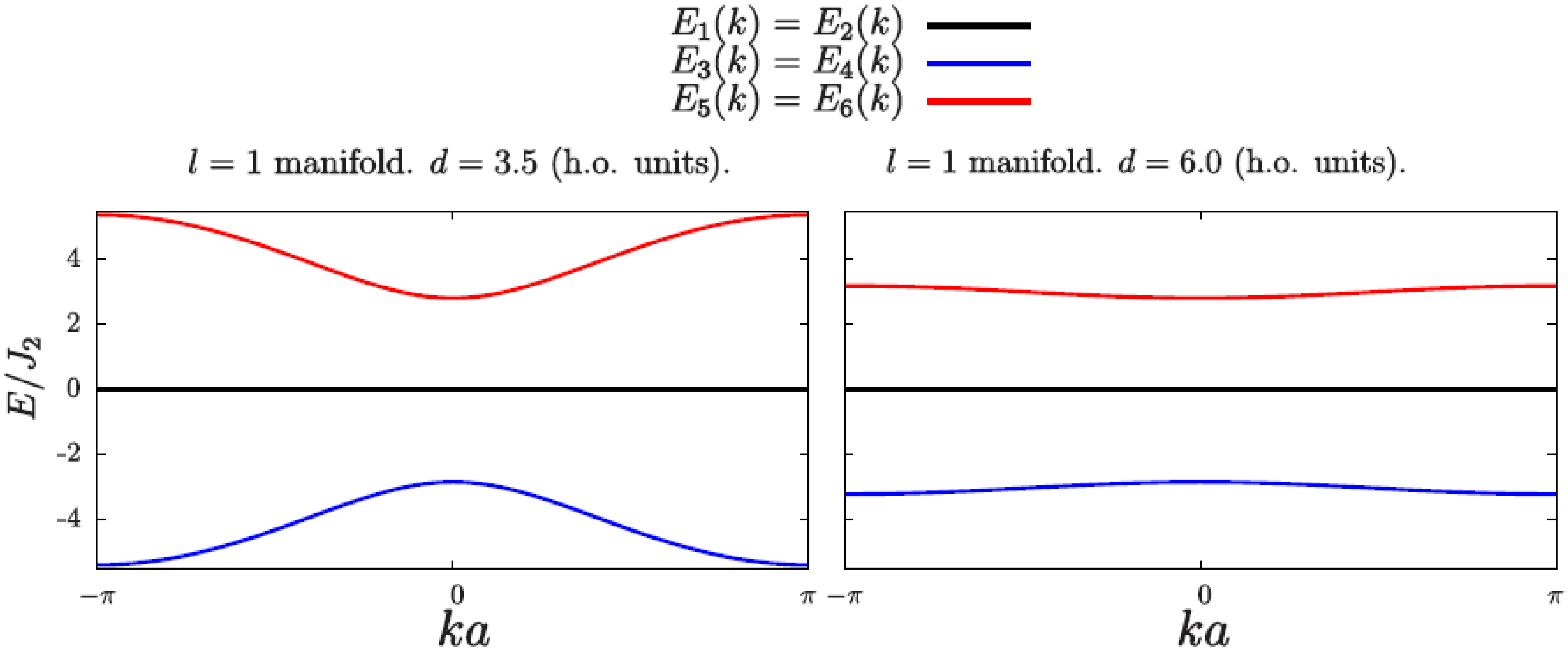

Gap of size $2\sqrt{2}J_2$ and all bands dispersionless in the limit $J_2 = J_3$

A lattice of rings for quantum simulation

- Exact diagonalization

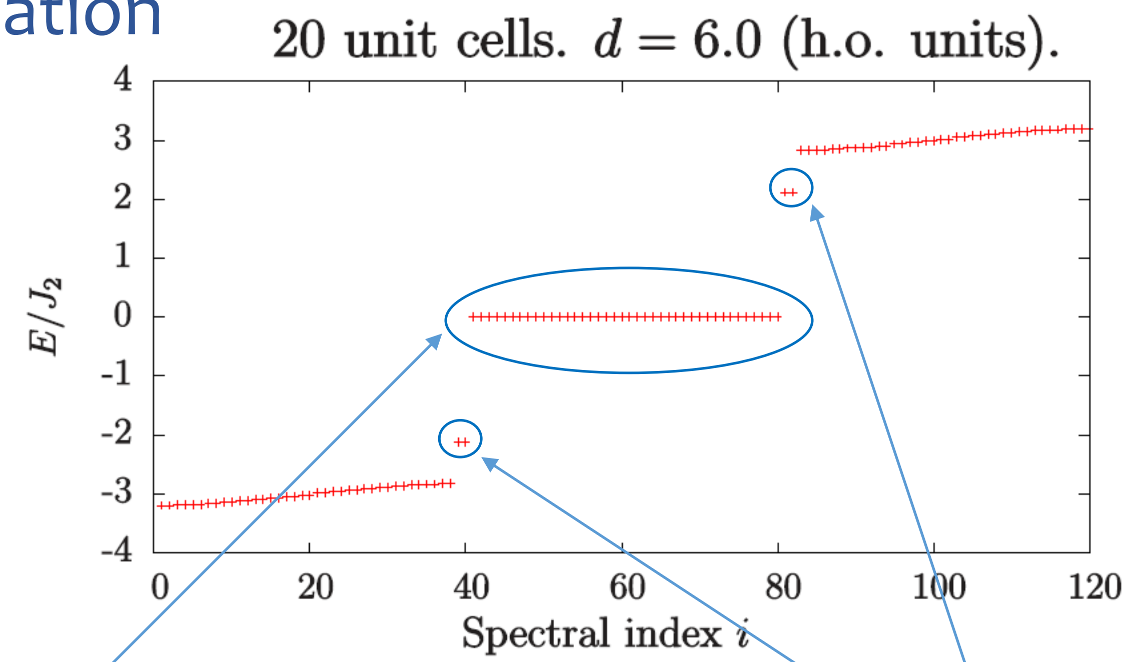

Flat band states, with no population on the A states

In-gap states, localized at the right edge and topologically non-trivial

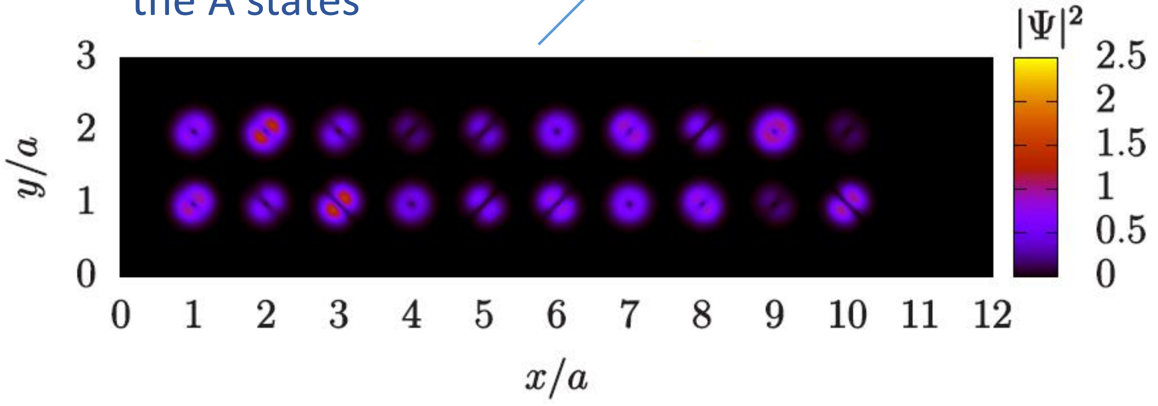

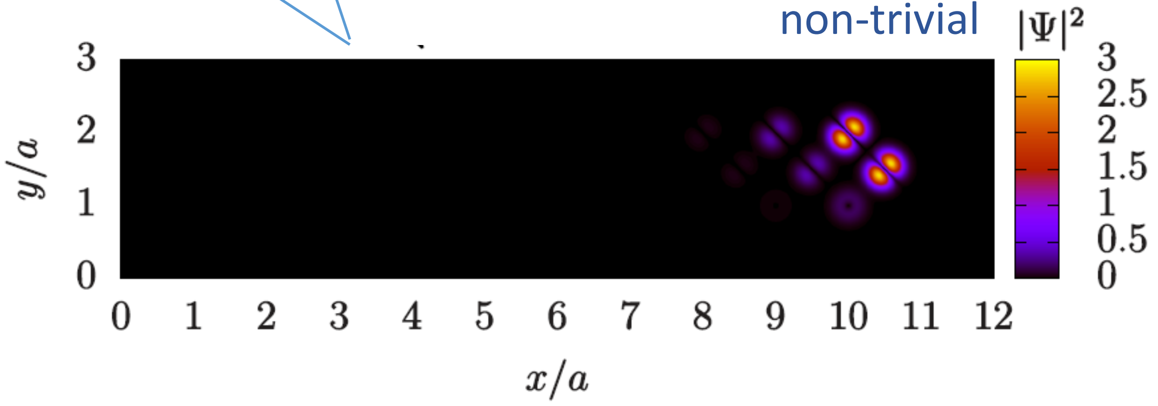

A lattice of rings for quantum simulation

A basis rotation decouples the model into two identical diamond chains with one state per site

$$|D_i\pm\rangle = \frac{1}{\sqrt{2}}(|C_i+\rangle \pm |B_i+\rangle)$$

$$|F_i\pm\rangle = \frac{1}{\sqrt{2}}(|C_i-\rangle \pm |B_i-\rangle)$$

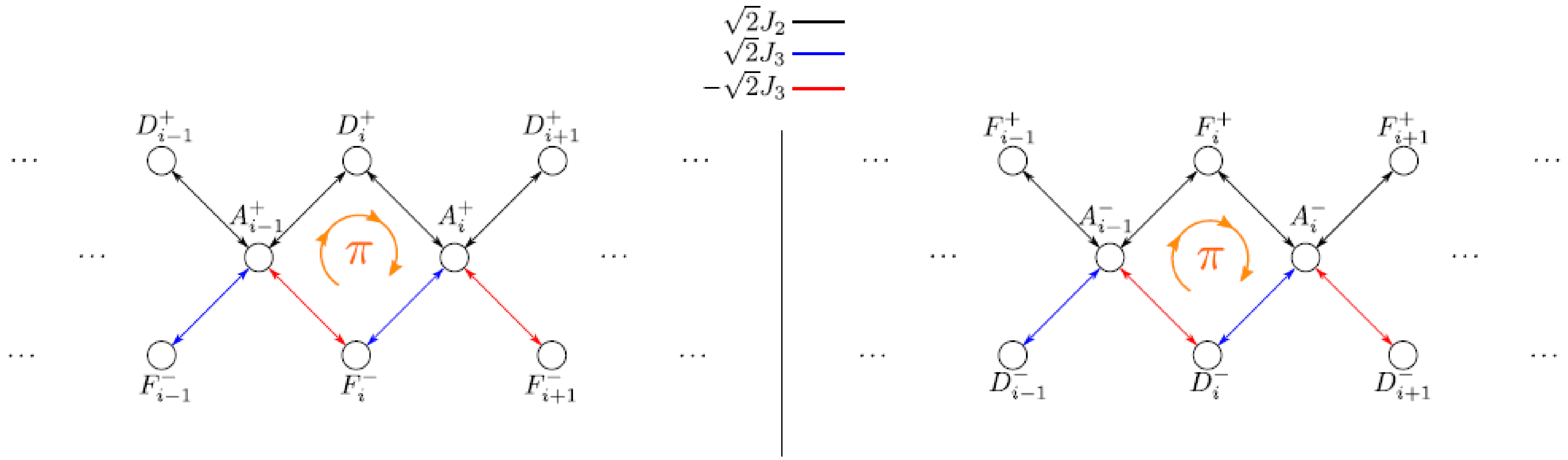

- The decoupling into two identical chains explains the degeneracy in the original model.
- The net π flux through the plaquettes accounts for the gap opening [1].

[1] A. A. Lopes and R. G. Dias, Phys. Rev. B **84**, 085124 (2011).

A lattice of rings for quantum simulation

By performing a second basis rotation, the system is further mapped into a modified Su-Schrieffer-Hegger (SSH) model (similar mapping for the A⁻ chain)

$$|G_i+\rangle = \frac{1}{\sqrt{J_2^2 + J_3^2}}(J_2|D_i+\rangle + J_3|F_i-\rangle)$$

$$|G_i-\rangle = \frac{1}{\sqrt{J_2^2 + J_3^2}}(J_3|D_i+\rangle - J_2|F_i-\rangle)$$

Example with 3 cells

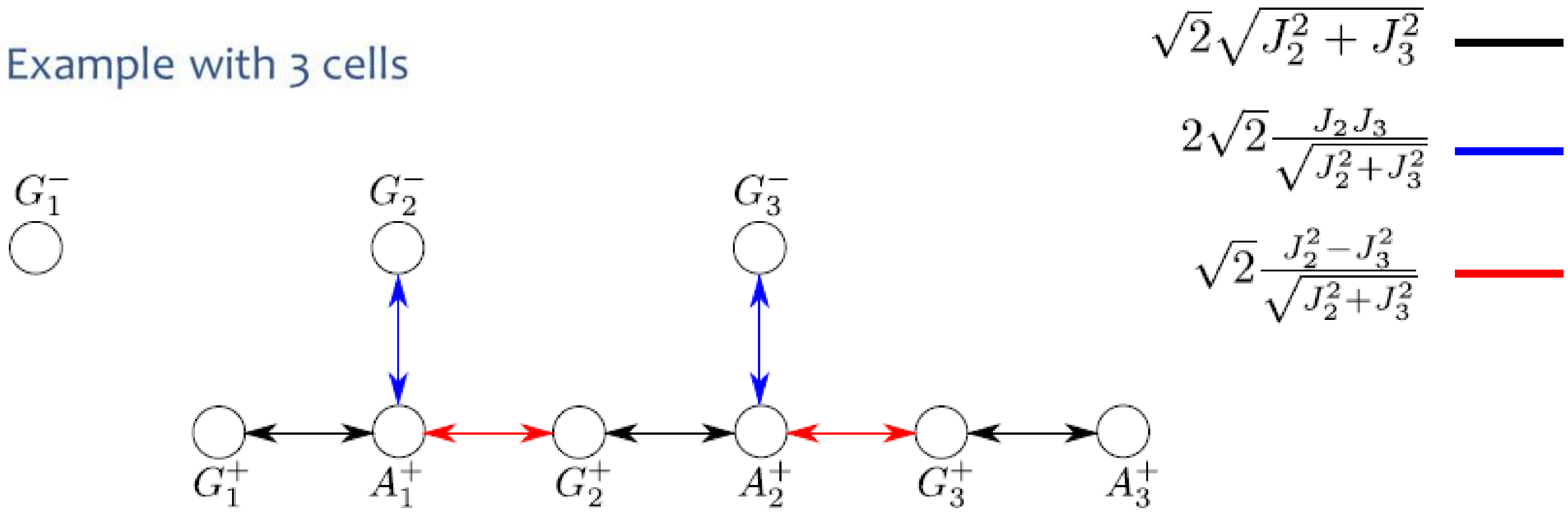

A lattice of rings for quantum simulation

Example with 3 cells

Limit $J_2 = J_3 \equiv J$

Zero-energy bulk state:

$\frac{1}{\sqrt{2}}(|G_2+\rangle - |G_3-\rangle)$

$2J$

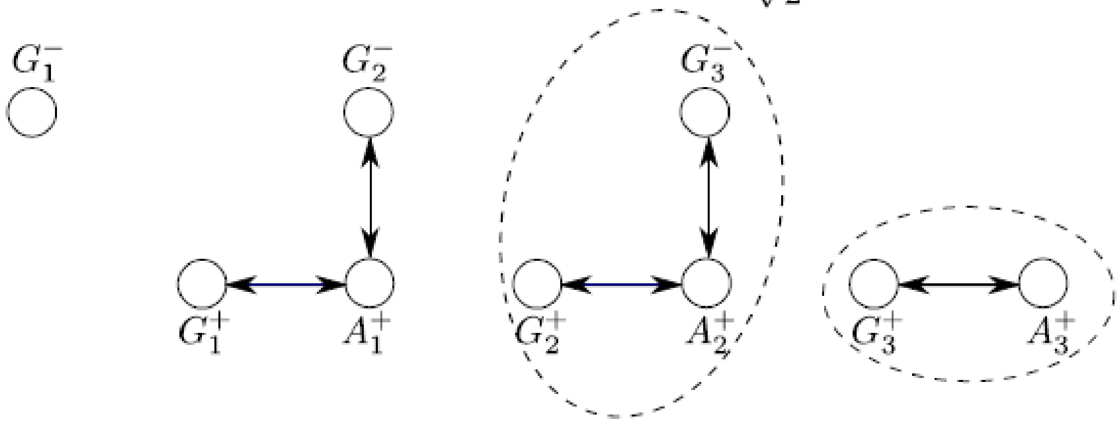

Topological edge states:

$\frac{1}{\sqrt{2}}(|G_3+\rangle + |A_3+\rangle) \rightarrow E = 2J$

$\frac{1}{\sqrt{2}}(|G_3+\rangle - |A_3+\rangle) \rightarrow E = -2J$

- The topological nature of the edge states can be shown by performing a third mapping to a diamond chain with alternating hoppings [1].
- Topological edge states persist in the entire $J_2 \neq J_3$ domain (except for the gap closing points $J_2/ J_3 = 0$)
- Zero-energy states can also be constructed in the case.
- In the limit $J_2 = J_3$, there is Aharanov-Bohm caging [2].
- This system is an example of square-root topological insulator [3].

[1] A. M. Marques and R. G. Dias, J. Phys.: Condens. Matter **30**, 305601 (2018)
[2] J. Vidal, R. Mosseri, and B. Douçot, Phys. Rev. Lett. **81**, 5888 (1998)
[3] M. Kremer *et al.*, arXiv:1805.05209

A lattice of rings for quantum simulation

- Aharanov-Bohm caging

Spatial confinement of initial wave packets composed of states $|A_i, \pm\rangle$ due to quantum interference

For $J_2 = J_3$

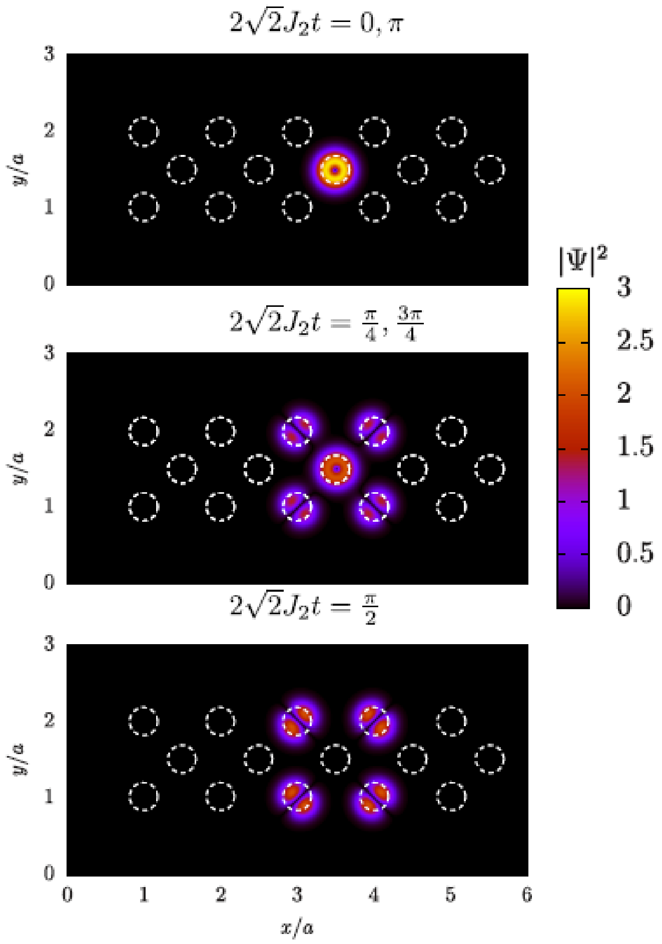

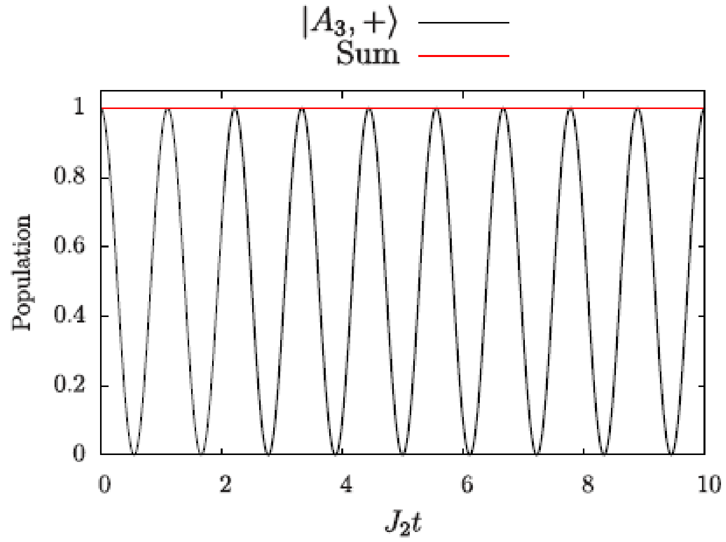

CONCLUSIONS

Ultracold atoms carrying OAM in ring traps constitute a very interesting platform for quantum sensing and quantum simulation (topology).

Examples:

Quantum sensing of non-linear interactions, magnetic fields, and rotations with an imbalanced superposition of the OAM modes of a BEC

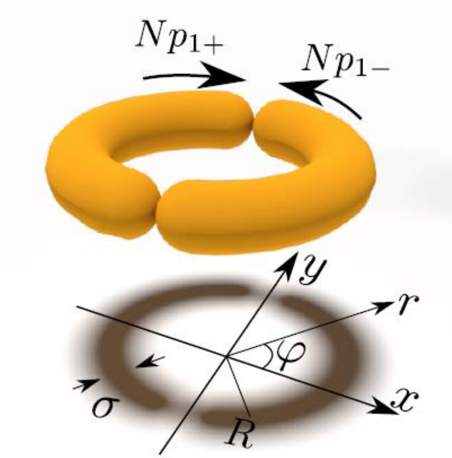

Complex tunnelings due to OAM states gives rise to non-trivial topology and dynamics (edge states and Aharanov-Bohm caging) in lattices of rings

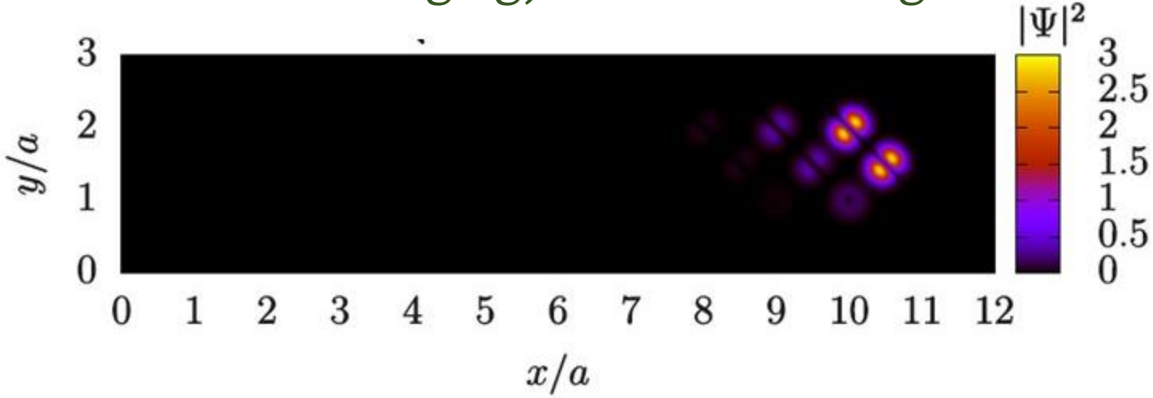

On progress:

- Interacting bosons in the Mott regime in a quasi 1D diamond lattice
- Corner states in 2D optical lattices

Thank you for your attention!